PERGAMON

International Journal of Solids and Structures 39 (2002) 4905–4925

INTERNATIONAL JOURNAL OF SOLIDS and STRUCTURES

www.elsevier.com/locate/ijsolstr

Anisotropic elastic plates with holes/cracks/inclusions subjected to out-of-plane bending moments

M.C. Hsieh, Chyanbin Hwu *

Institute of Aeronautics and Astronautics, National Cheng Kung University, 70101 Tainan, Taiwan, ROC

Received 28 November 2001; received in revised form 6 May 2002

Abstract

The problems of anisotropic plates containing holes, cracks and/or inclusions have been studied extensively for two-dimensional deformations. Although the correspondence between the two-dimensional problems and the plate bending problems has been observed long time ago, without clarifying the involved mathematical details one still cannot get the solutions of the plate bending problems directly from the solutions of the corresponding two-dimensional problems. Based upon the correspondence relation, recently we developed a Stroh-like formalism for the bending theory of anisotropic plates. By this newly developed formalism, most of the relations for bending problems can be organized into the forms for two-dimensional problems. Thus, by using the Stroh-like formalism, the analytical solutions for problems of anisotropic plates with holes/cracks/inclusions subjected to out-of-plane bending moments can be obtained directly from the solutions of the corresponding two-dimensional problems. The stresses (or resultant bending moments) around the hole/crack/inclusion boundaries are also given explicitly in this paper. Since the explicit closed-form solutions for the present cases have not been found in the literature, comparison is made with some special cases of which the analytical solutions exist, which shows that our solutions are exact, simple and general.

Keywords: Anisotropic elasticity; Hole; Inclusion; Crack; Plate bending; Stroh formalism

1. Introduction

Although the hole/crack/inclusion problems are very important in engineering applications, most of the analytical solutions found in the literature are for two-dimensional problems. As far as the authors' knowledge, the only related analytical solutions found in the literature for the bending problems are obtained by Lekhnitskii (1938) and Lu and Mahrenholtz (1994). The former was obtained for the orthotropic plates weakened by a circular hole or inclusion, which was derived nearly 63 years ago using Lekhnitskii's complex variable method (Lekhnitskii, 1968). The latter was obtained for the general anisotropic plates containing a polygon-like hole, which was derived using the modified Stroh's complex variable formalism

* Corresponding author. Tel.: +886-6-27-57575x63662; fax: +886-6-23-89940.
E-mail address: chwu@mail.ncku.edu.tw (C. Hwu).

PII: S0020-7683(02)00335-9

(Lu and Mahrenholtz, 1994). While the latter solution should cover the results presented by the former solution, no verification and comparison have been provided. Due to the complexity and non-verification of the solutions provided by Lu and Mahrenholtz (1994) (actually the eigen-relation derived in their paper is incorrect, and hence all their following results are doubtful), it is necessary for us to find a simple, exact and general solution for this important problem.

Since the boundary conditions for the hole/crack/inclusion problems are not easy to be satisfied by using the conventional methods of plate bending theory (Szilard, 1985), most of the efforts are devoted in the complex variable methods (Lekhnitskii, 1968). Unlike the progress of two-dimensional problems, no major advancement about the complex variable methods in plate bending theory has been developed during these few decades. Recently, owing to the efforts of several researchers, the complex variable methods in anisotropic elasticity have reached a big step by connecting Lekhnitskii formulation and Stroh formalism (Suo, 1990; Hwu, 1996; Barnett and Kirchner, 1997; Ting, 1999; Yin, 2000a,b). However, still very few contributions have been made to the plate bending problems. Through our experience in two-dimensional anisotropic elasticity, recently we develop a Stroh-like formalism for the bending theory of anisotropic plates (Hwu, 2002a). In our formalism, the deflections, the moments and the transverse shear forces can all be expressed in complex matrix form. Moreover, by careful re-organization, a Stroh-like compact and elegant solution form has been formulated. Through this re-organization, most of the relations for the bending problems look very like the Stroh formalism for two-dimensional linear anisotropic elasticity. Hence, almost all the mathematical techniques developed for two-dimensional problems can lend to the plate bending problems. Borrowing from this analogy, simple analytical solutions for anisotropic plates with holes/cracks/inclusions subjected to out-of-plane bending moments are now obtained explicitly. Moreover, the stresses (or resultant bending moments) around the hole/crack/inclusion boundaries are also given explicitly in this paper.

2. Stroh-like formalism for the bending theory of anisotropic plates

In the bending theory of anisotropic plates, the governing equation (combining the Kirchoff plate assumptions, the equilibrium equations, the constitutive laws and the kinematic relations) can be expressed in terms of the mid-plane lateral deflection w as (Vinson and Sierakowski, 1986)

$$D_{11}\frac{\partial^4 w}{\partial x^4} + 4D_{16}\frac{\partial^4 w}{\partial x^3\,\partial y} + 2(D_{12}+2D_{66})\frac{\partial^4 w}{\partial x^2\,\partial y^2} + 4D_{26}\frac{\partial^4 w}{\partial x\,\partial y^3} + D_{22}\frac{\partial^4 w}{\partial y^4} = q, \tag{1}$$

where x–y–z is the commonly used Cartesian coordinate system, q is the lateral load distribution, and D_{ij} is the bending stiffness of the plate. The deflection w can be determined by solving this partial differential equation with the satisfaction of the boundary conditions for the considered problems. After finding the deflection, all the other physical values such as the in-plane displacements (u, v), bending moments (M_x, M_y, M_{xy}), transverse shear forces (Q_x, Q_y), and internal stresses $(\sigma_x, \sigma_y, \tau_{xy})$ can all be obtained through the use of their relations with the deflection.

Although it seems not difficult to get a general solution for the deflection to satisfy the governing equation (1), it is really not easy to find a solution satisfying the boundary conditions for the complicated geometrical boundaries by using the conventional methods introduced in most of the textbooks of plates such as (Szilard, 1985). In order to solve the problems with hole/crack/inclusion boundaries, a Stroh-like complex variable formalism for the bending theory of anisotropic plates (Hwu, 2002a) will be used in this paper. In this formalism, the general solutions satisfying the governing equation (1) can be expressed as follows

$$w = w_0 + 2\mathrm{Re}\{c_1 w_1(z_1) + c_2 w_2(z_2)\}, \tag{2}$$

where Re stands for the real part of a complex number; w_0 is a particular solution of Eq. (1), whose form depends on the load distribution q on a plate surface; $w_1(z_1)$ and $w_2(z_2)$ are arbitrary analytic functions of complex variables

$$z_k = x + \mu_k y, \quad k = 1, 2, \tag{3}$$

where μ_k, $k = 1, 2$, are the material eigenvalues which have been assumed to be distinct in the general expression (2). The determination of the material eigenvalues and their associated eigenvectors will be described later. The coefficients c_1 and c_2 will be defined after introducing the material eigenvectors.

By introducing the stress function vector $\boldsymbol{\phi}$ and the slope vector $\boldsymbol{\alpha}$ as

$$\boldsymbol{\phi} = \begin{Bmatrix} \phi_1 \\ \phi_2 \end{Bmatrix} = \begin{Bmatrix} -\int M_y \,\mathrm{d}x \\ -\int M_x \,\mathrm{d}y \end{Bmatrix}, \qquad \boldsymbol{\alpha} = \begin{Bmatrix} \alpha_1 \\ \alpha_2 \end{Bmatrix} = \begin{Bmatrix} -\dfrac{\partial w}{\partial y} \\ \dfrac{\partial w}{\partial x} \end{Bmatrix}, \tag{4}$$

and using the general solution (2), a Stroh-like formalism has been developed as (Hwu, 2002a)

$$\boldsymbol{\phi} = \boldsymbol{\phi}_0 + 2\mathrm{Re}\{\mathbf{A}\mathbf{w}'(z)\}, \qquad \boldsymbol{\alpha} = \boldsymbol{\alpha}_0 + 2\mathrm{Re}\{\mathbf{B}\mathbf{w}'(z)\}, \tag{5}$$

where $\boldsymbol{\phi}_0$ and $\boldsymbol{\alpha}_0$ are the particular solutions related to the lateral load distribution q; $\mathbf{w}'(z)$ is a function vector defined as

$$\mathbf{w}'(z) = \begin{Bmatrix} w_1'(z_1) \\ w_2'(z_2) \end{Bmatrix}, \tag{6}$$

in which the prime ($'$) denotes differentiation with respect to its argument z_k. μ_k, and $\mathbf{A}$, $\mathbf{B}$ are the material eigenvalues and eigenvector matrices, which can be determined from the following eigen-relation:

$$\mathbf{N}\xi = \mu\xi, \tag{7a}$$

where

$$\mathbf{N} = \begin{bmatrix} \mathbf{N}_1 & \mathbf{N}_2 \\ \mathbf{N}_3 & \mathbf{N}_1^{\mathrm{T}} \end{bmatrix}, \qquad \xi = \begin{Bmatrix} \mathbf{a} \\ \mathbf{b} \end{Bmatrix}, \tag{7b}$$

and

$$\mathbf{N}_1 = -\mathbf{T}^{-1}\mathbf{R}^{\mathrm{T}}, \quad \mathbf{N}_2 = \mathbf{T}^{-1} = \mathbf{N}_2^{\mathrm{T}}, \quad \mathbf{N}_3 = \mathbf{R}\mathbf{T}^{-1}\mathbf{R}^{\mathrm{T}} - \mathbf{Q} = \mathbf{N}_3^{\mathrm{T}}. \tag{7c}$$

In the above eigen-relation, the three 2×2 real matrices $\mathbf{Q}$, $\mathbf{R}$ and $\mathbf{T}$ are defined as

$$\mathbf{Q} = \begin{bmatrix} D_{22}^* & -\frac{1}{2}D_{26}^* \\ -\frac{1}{2}D_{26}^* & \frac{1}{4}D_{66}^* \end{bmatrix}, \quad \mathbf{R} = \begin{bmatrix} -\frac{1}{2}D_{26}^* & D_{12}^* \\ \frac{1}{4}D_{66}^* & -\frac{1}{2}D_{16}^* \end{bmatrix}, \quad \mathbf{T} = \begin{bmatrix} \frac{1}{4}D_{66}^* & -\frac{1}{2}D_{16}^* \\ -\frac{1}{2}D_{16}^* & D_{11}^* \end{bmatrix}, \tag{8}$$

in which D_{ij}^* is the components of the inverse bending stiffness matrix D_{ij}, i.e.,

$$\begin{bmatrix} D_{11}^* & D_{12}^* & D_{16}^* \\ D_{12}^* & D_{22}^* & D_{26}^* \\ D_{16}^* & D_{26}^* & D_{66}^* \end{bmatrix} = \mathbf{D}^{-1}. \tag{9}$$

It has been proved that the material eigenvalues μ_k cannot be real due to the positive definiteness of strain energy and they will appear in two pairs of complex conjugates (Lekhnitskii, 1968). If the eigenvalues are assumed to be distinct and are arranged in the order that μ_1 and μ_2 are those with positive imaginary parts, their associated eigenvectors will be independent of each other and the eigenvector matrices $\mathbf{A}$ and $\mathbf{B}$ are defined as

$$\mathbf{A} = [\,\mathbf{a}_1 \quad \mathbf{a}_2\,], \quad \mathbf{B} = [\,\mathbf{b}_1 \quad \mathbf{b}_2\,]. \tag{10}$$

For the convenience of readers' reference, the explicit expressions of the fundamental matrix $\mathbf{N}$ and the eigenvectors $\mathbf{a}_k$ and $\mathbf{b}_k$ obtained in Hwu (2002a) are listed below

$$\mathbf{N}_1 = \begin{bmatrix} \dfrac{-2D_{26}}{D_{22}} & -1 \\ \dfrac{D_{12}}{D_{22}} & 0 \end{bmatrix}, \quad \mathbf{N}_2 = \begin{bmatrix} 4D_{66} - \dfrac{4D_{26}^2}{D_{22}} & -2D_{16} + \dfrac{2D_{12}D_{26}}{D_{22}} \\ -2D_{16} + \dfrac{2D_{12}D_{26}}{D_{22}} & D_{11} - \dfrac{D_{12}^2}{D_{22}} \end{bmatrix}, \quad \mathbf{N}_3 = \begin{bmatrix} \dfrac{-1}{D_{22}} & 0 \\ 0 & 0 \end{bmatrix}, \tag{11}$$

and

$$\mathbf{a}_k = c_k \begin{Bmatrix} h_k \\ g_k \end{Bmatrix}, \qquad \mathbf{b}_k = c_k \begin{Bmatrix} -\mu_k \\ 1 \end{Bmatrix}, \tag{12a}$$

where

$$h_k = D_{12} + D_{22}\mu_k^2 + 2D_{26}\mu_k, \quad g_k = \frac{D_{11}}{\mu_k} + D_{12}\mu_k + 2D_{16}, \tag{12b}$$

$$c_k^2 = \frac{1}{2(g_k - \mu_k h_k)}, \quad k = 1, 2. \tag{12c}$$

3. Moments and transverse shear forces

In practical applications, one is usually interested in the moments and shear forces around the hole boundary since most of the critical stress occurs along the hole boundary. To find the moments and transverse shear forces around the hole boundary, the conventional way is to calculate the moments (M_x, M_y, M_{xy}) and transverse shear forces (Q_x, Q_y) or effective transverse shear forces (V_x, V_y) by using their relations with the deflection w, then use the transformation law to find their values in the normal and tangent coordinate system, i.e. M_n, M_t, M_{nt}, Q_n, Q_t, V_n, V_t. Since in our newly developed Stroh-like formalism, the final results are expressed in terms of the stress function vector $\boldsymbol{\phi}$ and slope vector $\boldsymbol{\alpha}$, it is hoped that the moments and the transverse shear forces can be found directly from $\boldsymbol{\phi}$ instead of using the conventional way. To achieve this goal, let us consider the equilibrium equation with $q = 0$, i.e.,

$$\frac{\partial Q_x}{\partial x} + \frac{\partial Q_y}{\partial y} = 0, \qquad \frac{\partial M_x}{\partial x} + \frac{\partial M_{xy}}{\partial y} - Q_x = 0, \qquad \frac{\partial M_{xy}}{\partial x} + \frac{\partial M_y}{\partial y} - Q_y = 0. \tag{13}$$

The first equation of (13) will be satisfied automatically if we let

$$Q_x = -\frac{\partial \eta}{\partial y}, \qquad Q_y = \frac{\partial \eta}{\partial x}. \tag{14}$$

From the definition of the stress function vector $\boldsymbol{\phi}$ given in (4, part 1), we know

$$M_x = -\frac{\partial \phi_2}{\partial y}, \qquad M_y = -\frac{\partial \phi_1}{\partial x}. \tag{15}$$

Substituting (14) and (15) into (13, parts 2 and 3), we obtain

$$M_{xy} = \frac{\partial \phi_2}{\partial x} - \eta = \frac{\partial \phi_1}{\partial y} + \eta. \tag{16}$$

The second equality of (16) will then lead to

$$\eta = \frac{1}{2}\left(\frac{\partial \phi_2}{\partial x} - \frac{\partial \phi_1}{\partial y}\right). \tag{17}$$

Like the surface traction for two-dimensional problems, we may now define the surface moments along the hole boundary, M_1 and M_2, as

$$M_1 = M_x \cos\theta + M_{xy} \sin\theta, \qquad M_2 = M_{xy} \cos\theta + M_y \sin\theta, \tag{18a}$$

and the surface moments along the surface perpendicular to the hole boundary, M_1^* and M_2^*, as

$$M_1^* = -M_x \sin\theta + M_{xy} \cos\theta, \qquad M_2^* = -M_{xy} \sin\theta + M_y \cos\theta, \tag{18b}$$

in which

$$\cos\theta = n_1 = \frac{\partial y}{\partial s} = \frac{\partial x}{\partial n}, \qquad \sin\theta = n_2 = -\frac{\partial x}{\partial s} = \frac{\partial y}{\partial n}, \tag{18c}$$

where θ denotes the angle between the normal n- and x-axis (see Fig. 1). Substituting (15) and (16) into (18a)–(18c) and using chain rule for differentiation, the surface moment M_i and M_i^*, $i = 1, 2$ can then be expressed as

$$M_1 = -\frac{\partial \phi_2}{\partial s} + \eta \frac{\partial x}{\partial s}, \qquad M_2 = \frac{\partial \phi_1}{\partial s} + \eta \frac{\partial y}{\partial s}, \tag{19a}$$

$$M_1^* = \frac{\partial \phi_2}{\partial n} - \eta \frac{\partial x}{\partial n}, \qquad M_2^* = -\frac{\partial \phi_1}{\partial n} - \eta \frac{\partial y}{\partial n}. \tag{19b}$$

The values in the n–t coordinate can be calculated from the values in the x–y coordinate according to the following transformation laws:

$$\begin{aligned}
M_n &= M_1 \cos\theta + M_2 \sin\theta = \cos^2\theta M_x + \sin^2\theta M_y + 2\sin\theta\cos\theta M_{xy}, \\
M_{nt} &= -M_1 \sin\theta + M_2 \cos\theta = M_1^* \cos\theta + M_2^* \sin\theta = \sin\theta\cos\theta(M_y - M_x) + (\cos^2\theta - \sin^2\theta)M_{xy}, \\
M_t &= -M_1^* \sin\theta + M_2^* \cos\theta = \sin^2\theta M_x + \cos^2\theta M_y - 2\sin\theta\cos\theta M_{xy},
\end{aligned} \tag{20}$$

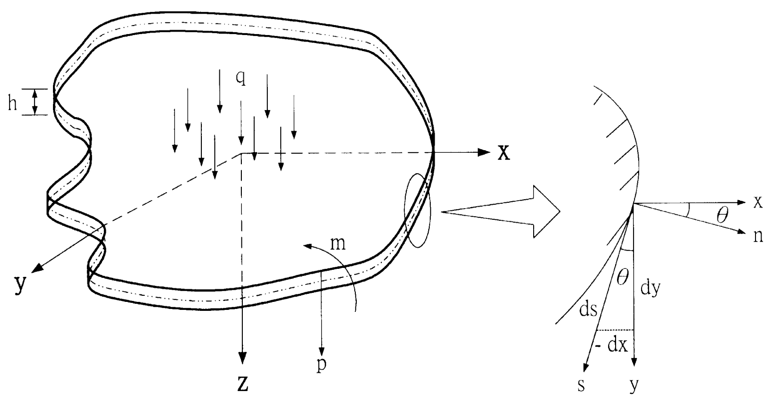

Fig. 1. Plate geometry.

$$Q_n = \cos\theta Q_x + \sin\theta Q_y,$$
$$Q_t = -\sin\theta Q_x + \cos\theta Q_y.$$

Substituting (19a) and (19b) into (20) and using (18c), the moments M_n, M_{nt}, M_t can be written as

$$\begin{aligned} M_n &= \frac{\partial\phi_1}{\partial s}\sin\theta - \frac{\partial\phi_2}{\partial s}\cos\theta, \\ M_{nt} &= \frac{\partial\phi_1}{\partial s}\cos\theta + \frac{\partial\phi_2}{\partial s}\sin\theta + \eta = -\frac{\partial\phi_1}{\partial n}\sin\theta + \frac{\partial\phi_2}{\partial n}\cos\theta - \eta, \\ M_t &= -\frac{\partial\phi_1}{\partial n}\cos\theta - \frac{\partial\phi_2}{\partial n}\sin\theta, \end{aligned} \tag{21}$$

or in matrix notation

$$\begin{aligned} M_n &= -\mathbf{s}^{\mathrm{T}}\boldsymbol{\phi}_{,s}, \\ M_{nt} &= \mathbf{n}^{\mathrm{T}}\boldsymbol{\phi}_{,s} + \eta = \mathbf{s}^{\mathrm{T}}\boldsymbol{\phi}_{,n} - \eta, \\ M_t &= -\mathbf{n}^{\mathrm{T}}\boldsymbol{\phi}_{,n}, \end{aligned} \tag{22a}$$

where the comma denotes differentiation and

$$\mathbf{s}^{\mathrm{T}} = [\,-\sin\theta \quad \cos\theta\,], \quad \mathbf{n}^{\mathrm{T}} = [\,\cos\theta \quad \sin\theta\,]. \tag{22b}$$

From (22a, part 2), we obtain

$$\eta = \frac{1}{2}\left(\mathbf{s}^{\mathrm{T}}\boldsymbol{\phi}_{,n} - \mathbf{n}^{\mathrm{T}}\boldsymbol{\phi}_{,s}\right), \tag{23}$$

so that the moment M_{nt} can also be expressed as

$$M_{nt} = \frac{1}{2}\left(\mathbf{s}^{\mathrm{T}}\boldsymbol{\phi}_{,n} + \mathbf{n}^{\mathrm{T}}\boldsymbol{\phi}_{,s}\right). \tag{24}$$

Substituting (14) into (20, parts 4 and 5) and using (18c) and the chain rule for differentiation, the transverse shear forces Q_n and Q_t can now be expressed as

$$Q_n = -\eta_{,s}, \quad Q_t = \eta_{,n}, \tag{25}$$

Substituting (23) into (25), we have

$$Q_n = -\frac{1}{2}\left(\mathbf{s}^{\mathrm{T}}\boldsymbol{\phi}_{,ns} - \mathbf{n}^{\mathrm{T}}\boldsymbol{\phi}_{,ss}\right), \quad Q_t = \frac{1}{2}\left(\mathbf{s}^{\mathrm{T}}\boldsymbol{\phi}_{,nn} - \mathbf{n}^{\mathrm{T}}\boldsymbol{\phi}_{,sn}\right). \tag{26}$$

With the results of (24) and (26), the effective transverse shear forces V_n and V_t can be found to be

$$V_n = Q_n + \frac{\partial M_{nt}}{\partial s} = \mathbf{n}^{\mathrm{T}}\boldsymbol{\phi}_{,ss}, \quad V_t = Q_t + \frac{\partial M_{nt}}{\partial n} = \mathbf{s}^{\mathrm{T}}\boldsymbol{\phi}_{,nn}. \tag{27}$$

In summary, from (22a), (22b), (24), (26) and (27), we see that all of the moments and transverse shear forces and effective transverse shear forces in the normal-tangent coordinate have simple relations with the stress function vector $\boldsymbol{\phi}$.

4. Some identities

In Stroh formalism for two-dimensional problems, there are many identities converting certain combinations of eigenvalues and eigenvectors which are complex values to real quantities directly obtainable from the elastic constants. By using these identities, many complex form solutions can be converted to real form solutions. Since all the physical quantities are real, the real form solutions are more suitable for the engineering application. To achieve this goal, some identities which are useful for the present paper will be derived in this section.

For two-dimensional problems, most of the identities are derived from the eigen-relation like (7a)–(7c) for the plate bending problems. Following the approach for the two-dimensional problems (Ting, 1996), we re-organize the eigen-relation (7a)–(7c) as

$$\mathbf{N}\begin{bmatrix}\mathbf{A}\\ \mathbf{B}\end{bmatrix} = \begin{bmatrix}\mathbf{A}\\ \mathbf{B}\end{bmatrix}\langle\mu_k\rangle, \tag{28}$$

where $\langle\mu_k\rangle$ denotes a diagonal matrix whose diagonal components are μ_k, $k = 1, 2$. Postmultiplying both sides of (28) by $[\mathbf{A}^{-1}\mathbf{B}^{-1}]$, we obtain

$$\mathbf{N}\begin{bmatrix}\mathbf{I} & \mathbf{AB}^{-1}\\ \mathbf{BA}^{-1} & \mathbf{I}\end{bmatrix} = \begin{bmatrix}\mathbf{A}\langle\mu_k\rangle\mathbf{A}^{-1} & \mathbf{A}\langle\mu_k\rangle\mathbf{B}^{-1}\\ \mathbf{B}\langle\mu_k\rangle\mathbf{A}^{-1} & \mathbf{B}\langle\mu_k\rangle\mathbf{B}^{-1}\end{bmatrix}, \tag{29}$$

where $\mathbf{AB}^{-1}$ and $\mathbf{BA}^{-1}$ can be expressed in terms of three fundamental real matrices, $\mathbf{S}$, $\mathbf{H}$ and $\mathbf{L}$ as

$$\begin{aligned}\mathbf{AB}^{-1} &= \mathbf{AB}^{\mathrm{T}}(\mathbf{BB}^{\mathrm{T}})^{-1} = -(\mathbf{S} + \mathrm{i}\mathbf{I})\mathbf{L}^{-1},\\ \mathbf{BA}^{-1} &= \mathbf{BA}^{\mathrm{T}}(\mathbf{AA}^{\mathrm{T}})^{-1} = (\mathbf{S}^{\mathrm{T}} + \mathrm{i}\mathbf{I})\mathbf{H}^{-1},\end{aligned} \tag{30}$$

where $\mathbf{S}$, $\mathbf{H}$ and $\mathbf{L}$ are defined as

$$\mathbf{S} = \mathrm{i}(2\mathbf{AB}^{\mathrm{T}} - \mathbf{I}), \quad \mathbf{H} = 2\mathrm{i}\mathbf{AA}^{\mathrm{T}}, \quad \mathbf{L} = -2\mathrm{i}\mathbf{BB}^{\mathrm{T}}. \tag{31}$$

These three fundamental matrices can be proved to be real through the orthogonality relation between the eigenvectors $\mathbf{A}$ and $\mathbf{B}$ (Hwu, 2002a). Substituting (30) into (29) and using the expression given in (7b) for $\mathbf{N}$, we obtain the following identities

$$\begin{aligned}\mathbf{A}\langle\mu_k\rangle\mathbf{A}^{-1} &= \mathbf{N}_1 + \mathbf{N}_2\mathbf{S}^{\mathrm{T}}\mathbf{H}^{-1} + \mathrm{i}\mathbf{N}_2\mathbf{H}^{-1},\\ \mathbf{A}\langle\mu_k\rangle\mathbf{B}^{-1} &= \mathbf{N}_2 - \mathbf{N}_1\mathbf{S}\mathbf{L}^{-1} - \mathrm{i}\mathbf{N}_1\mathbf{L}^{-1},\\ \mathbf{B}\langle\mu_k\rangle\mathbf{B}^{-1} &= \mathbf{N}_1^{\mathrm{T}} - \mathbf{N}_3\mathbf{S}\mathbf{L}^{-1} - \mathrm{i}\mathbf{N}_3\mathbf{L}^{-1}.\end{aligned} \tag{32}$$

From the above derivation, we see that the identities (32) are associated with the eigen-relation (7a)–(7c). Therefore, if the eigen-relation is generalized, generalized identities of (32) can also be obtained automatically. Like the generalized eigen-relation for the two-dimensional problems (Ting, 1996), the eigen-relation (7a)–(7c) can be generalized as

$$\mathbf{N}(\theta)\xi = \mu(\theta)\xi, \tag{33a}$$

where

$$\mathbf{N}(\theta) = \begin{bmatrix}\mathbf{N}_1(\theta) & \mathbf{N}_2(\theta)\\ \mathbf{N}_3(\theta) & \mathbf{N}_1^{\mathrm{T}}(\theta)\end{bmatrix}, \quad \xi = \begin{Bmatrix}\mathbf{a}\\ \mathbf{b}\end{Bmatrix}, \tag{33b}$$

and

$$\mathbf{N}_1(\theta) = -\mathbf{T}^{-1}(\theta)\mathbf{R}^{\mathrm{T}}(\theta), \quad \mathbf{N}_2(\theta) = \mathbf{T}^{-1}(\theta) = \mathbf{N}_2^{\mathrm{T}}(\theta), \quad \mathbf{N}_3(\theta) = \mathbf{R}(\theta)\mathbf{T}^{-1}(\theta)\mathbf{R}^{\mathrm{T}}(\theta) - \mathbf{Q}(\theta) = \mathbf{N}_3^{\mathrm{T}}(\theta). \tag{33c}$$

In (33c), $\mathbf{Q}(\theta)$, $\mathbf{R}(\theta)$ and $\mathbf{T}(\theta)$ are related to the matrices $\mathbf{Q}$, $\mathbf{R}$ and $\mathbf{T}$ defined in (8) by

$$\begin{aligned}\mathbf{Q}(\theta) &= \mathbf{Q}\cos^2\theta + (\mathbf{R} + \mathbf{R}^{\mathrm{T}})\sin\theta\cos\theta + \mathbf{T}\sin^2\theta,\\ \mathbf{R}(\theta) &= \mathbf{R}\cos^2\theta + (\mathbf{T} - \mathbf{Q})\sin\theta\cos\theta - \mathbf{R}^{\mathrm{T}}\sin^2\theta,\\ \mathbf{T}(\theta) &= \mathbf{T}\cos^2\theta - (\mathbf{R} + \mathbf{R}^{\mathrm{T}})\sin\theta\cos\theta + \mathbf{Q}\sin^2\theta.\end{aligned} \tag{34}$$

Same as the two-dimensional problems (Ting, 1996), the eigenvalue $\mu(\theta)$ of (33a) is related to the eigenvalue μ of (7a) by

$$\mu(\theta) = \frac{-\sin\theta + \mu\cos\theta}{\cos\theta + \mu\sin\theta}. \tag{35}$$

Using (33a)–(33c) and following the same procedures for the derivation of the identities (32), we can obtain the generalized identities of (32) as

$$\mathbf{A}\langle\mu_k(\theta)\rangle\mathbf{A}^{-1} = \mathbf{E}_1(\theta) + \mathrm{i}\mathbf{F}_1(\theta), \tag{36a}$$

$$\mathbf{A}\langle\mu_k(\theta)\rangle\mathbf{B}^{-1} = \mathbf{E}_2(\theta) + \mathrm{i}\mathbf{F}_2(\theta), \tag{36b}$$

$$\mathbf{B}\langle\mu_k(\theta)\rangle\mathbf{B}^{-1} = \mathbf{E}_3(\theta) + \mathrm{i}\mathbf{F}_3(\theta), \tag{36c}$$

where

$$\begin{aligned}
&\mathbf{E}_1(\theta) = \mathbf{N}_1(\theta) + \mathbf{N}_2(\theta)\mathbf{S}^{\mathrm{T}}\mathbf{H}^{-1}, \quad \mathbf{F}_1(\theta) = \mathbf{N}_2(\theta)\mathbf{H}^{-1},\\
&\mathbf{E}_2(\theta) = \mathbf{N}_2(\theta) - \mathbf{N}_1(\theta)\mathbf{S}\mathbf{L}^{-1}, \quad \mathbf{F}_2(\theta) = -\mathbf{N}_1(\theta)\mathbf{L}^{-1},\\
&\mathbf{E}_3(\theta) = \mathbf{N}_1^{\mathrm{T}}(\theta) - \mathbf{N}_3(\theta)\mathbf{S}\mathbf{L}^{-1}, \quad \mathbf{F}_3(\theta) = -\mathbf{N}_3(\theta)\mathbf{L}^{-1}.
\end{aligned} \tag{37}$$

Since $\mathbf{N}_i(0) = \mathbf{N}_i$ and $\mu(0) = \mu$, the identities (32) are just special cases of identities (36a)–(36c).

When the identities (32) and (36a)–(36c) are applied, the solutions containing the *complex* matrices **A**, **B** and $\langle\mu_k(\theta)\rangle$ may then be expressed in terms of the *real* matrices $\mathbf{N}_i(\theta)$, **S**, **H** and **L**. From the definitions of $\mathbf{N}_i(\theta)$ and **S**, **H** and **L** given in (33c) and (31), we know that they are related to the bending stiffnesses D_{ij}. By referring to the procedures of finding $\mathbf{N}_i$, **S**, **H** and **L** for the two-dimensional problems (Ting, 1996), we have found the explicit expressions of $\mathbf{N}_i(\theta)$, **S**, **H** and **L** for the plate bending problems (Hsieh and Hwu, 2002a), which would be helpful for the present problems.

5. Elliptical holes

Consider an unbounded anisotropic plate weakened by an elliptical hole subjected to out-of-plane bending moments $M_x = \widehat{M}_x$, $M_y = \widehat{M}_y$, and $M_{xy} = 0$ at infinity (Fig. 2). There is no load around the edge of the elliptical hole. The contour of the elliptical hole is represented by

$$x = a\cos\psi, \quad y = b\sin\psi, \tag{38}$$

where $2a$, $2b$ are the major and minor axes of the ellipse and ψ is a real parameter. The boundary conditions of this problem can be expressed as

$$M_x = \widehat{M}_x, \quad M_y = \widehat{M}_y, \quad M_{xy} = 0 \quad \text{at infinity}, \tag{39a}$$

$$M_n = V_n = 0 \quad \text{along the hole boundary}. \tag{39b}$$

Since the boundary considered in this problem is an elliptical boundary, it is not easy to find a solution satisfying (39b) due to the complexity of describing the normal direction n. The substitutes of the boundary conditions, which are suitable for the Stroh-like formalism, have been discussed in Hwu (2002a). From the discussions of Hwu (2002a), we know that the boundary condition (39a) and (39b) can be expressed in terms of the stress function as

$$\boldsymbol{\phi} = -\widehat{M}_x y\mathbf{i}_2 - \widehat{M}_y x\mathbf{i}_1 \quad \text{at infinity}, \tag{40a}$$

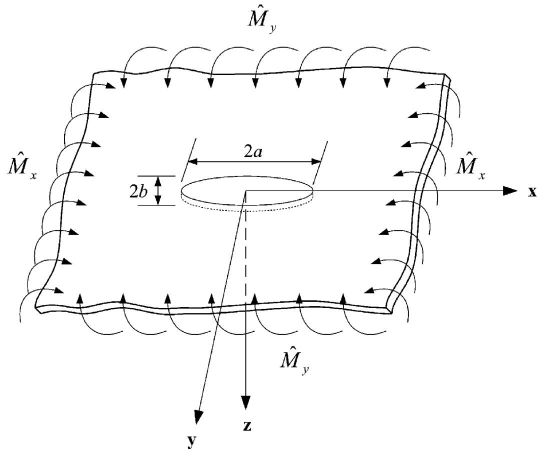

Fig. 2. An anisotropic plate weakened by an elliptical hole subjected to out-of-plane bending moments $\widehat{M}_x$ and $\widehat{M}_y$.

$$\boldsymbol{\phi} = 0 \quad \text{along the hole boundary,} \tag{40b}$$

where

$$\mathbf{i}_1 = \begin{Bmatrix} 1 \\ 0 \end{Bmatrix}, \quad \mathbf{i}_2 = \begin{Bmatrix} 0 \\ 1 \end{Bmatrix}. \tag{40c}$$

Since there is no lateral load applied on the plate, i.e., $q = 0$, the particular solutions $\boldsymbol{\phi}_0$ and $\boldsymbol{\alpha}_0$ of (5) are set to zero. In order to satisfy the boundary condition at infinity, we add the stress function vector $\boldsymbol{\phi}^\infty$ and the slope vector $\boldsymbol{\alpha}^\infty$ to the general solution (5). Thus, the solution to this problem can be expressed as

$$\boldsymbol{\phi} = \boldsymbol{\phi}^\infty + 2\mathrm{Re}\{\mathbf{A}\mathbf{w}'(z)\}, \tag{41a}$$

$$\boldsymbol{\alpha} = \boldsymbol{\alpha}^\infty + 2\mathrm{Re}\{\mathbf{B}\mathbf{w}'(z)\}, \tag{41b}$$

where

$$\boldsymbol{\phi}^\infty = -\widehat{M}_x y \mathbf{i}_2 - \widehat{M}_y x \mathbf{i}_1, \quad \boldsymbol{\alpha}^\infty = \widehat{M}_x(\mathbf{d}_2 y - \mathbf{d}_1 x) + \widehat{M}_y(\mathbf{d}_4 y - \mathbf{d}_3 x), \tag{42a}$$

and

$$\mathbf{d}_1 = \begin{Bmatrix} -D_{16}^*/2 \\ D_{11}^* \end{Bmatrix}, \quad \mathbf{d}_2 = \begin{Bmatrix} D_{12}^* \\ -D_{16}^*/2 \end{Bmatrix}, \quad \mathbf{d}_3 = \begin{Bmatrix} -D_{26}^*/2 \\ D_{12}^* \end{Bmatrix}, \quad \mathbf{d}_4 = \begin{Bmatrix} D_{22}^* \\ -D_{26}^*/2 \end{Bmatrix}. \tag{42b}$$

In Eqs. (42a) and (42b), $\boldsymbol{\phi}^\infty$ is selected to match the boundary condition at infinity; $\boldsymbol{\alpha}^\infty$ can be obtained by integrating the following constitutive relation

$$-\begin{Bmatrix} \dfrac{\partial^2 w}{\partial x^2} \\ \dfrac{\partial^2 w}{\partial y^2} \\ 2\dfrac{\partial^2 w}{\partial x \partial y} \end{Bmatrix} = \begin{bmatrix} D_{11}^* & D_{12}^* & D_{16}^* \\ D_{12}^* & D_{22}^* & D_{26}^* \\ D_{16}^* & D_{26}^* & D_{66}^* \end{bmatrix} \begin{Bmatrix} M_x \\ M_y \\ M_{xy} \end{Bmatrix}, \tag{43}$$

with $M_x = \widehat{M}_x$, $M_y = \widehat{M}_y$, and $M_{xy} = 0$.

In order to satisfy the free edge condition around the hole boundary shown in (40b), by referring to the solutions of the corresponding two-dimensional problems (Hwu and Yen, 1992; Hwu, 1992) we select

$$\mathbf{w}'(z) = \langle \varsigma_k^{-1} \rangle \mathbf{k}, \quad \varsigma_k = \frac{z_k + \sqrt{z_k^2 - a^2 - \mu_k^2 b^2}}{a - i\mu_k b}, \tag{44}$$

where $\mathbf{k}$ is the unknown coefficient to be determined through the satisfaction of the boundary condition. Substituting (3) and (38) into (44), we obtain

$$\mathbf{w}'(z) = \mathrm{e}^{-\mathrm{i}\psi} \mathbf{k} \quad \text{along the hole boundary.} \tag{45}$$

Substituting (45) and (42a, part 1) into (41a) with x and y given by (38), the free edge boundary condition (40b) now leads to

$$\mathbf{k} = \frac{1}{2} \mathbf{A}^{-1} \left(\mathrm{i}b\widehat{M}_x \mathbf{i}_2 + a\widehat{M}_y \mathbf{i}_1 \right). \tag{46}$$

Substituting (46) into (44), we obtain

$$\mathbf{w}'(z) = \frac{1}{2} \langle \varsigma_k^{-1} \rangle \mathbf{A}^{-1} \left(\mathrm{i}b\widehat{M}_x \mathbf{i}_2 + a\widehat{M}_y \mathbf{i}_1 \right). \tag{47a}$$

With the use of (12a, part 1), (10) and (40c), Eq. (47a) can be further expressed as

$$\mathbf{w}'(z) = \frac{1}{2d} \left\{ \begin{array}{c} \dfrac{-a\widehat{M}_y g_2 + \mathrm{i}b\widehat{M}_x h_2}{c_1 \varsigma_1} \\ \dfrac{a\widehat{M}_y g_1 - \mathrm{i}b\widehat{M}_x h_1}{c_2 \varsigma_2} \end{array} \right\}, \tag{47b}$$

where $d = h_2 g_1 - h_1 g_2$ and c_k, h_k, g_k, $k = 1, 2$ are defined in (12a)–(12c).

By combining (41a), (41b) and (47a), the explicit solution of the present problem can be expressed as

$$\begin{aligned} \boldsymbol{\phi} &= \boldsymbol{\phi}^\infty + \mathrm{Re}\left\{ \mathbf{A} \langle \varsigma_k^{-1} \rangle \mathbf{A}^{-1} \left(a\widehat{M}_y \mathbf{i}_1 + \mathrm{i}b\widehat{M}_x \mathbf{i}_2 \right) \right\}, \\ \boldsymbol{\alpha} &= \boldsymbol{\alpha}^\infty + \mathrm{Re}\left\{ \mathbf{B} \langle \varsigma_k^{-1} \rangle \mathbf{A}^{-1} \left(a\widehat{M}_y \mathbf{i}_1 + \mathrm{i}b\widehat{M}_x \mathbf{i}_2 \right) \right\}, \end{aligned} \tag{48}$$

where $\boldsymbol{\phi}^\infty$ and $\boldsymbol{\alpha}^\infty$ are given in (42a) and (42b). With the explicit solution found in (48), all the physical responses such as the deflection, bending moments and transverse shear forces of the plate can be obtained by using their relations with the slope vector and stress function vectors defined in (4), or using the results of (47a) and (47b) together with the expression (2) for the deflection then applying the relations between bending moments/transverse shear forces and deflections (Vinson and Sierakowski, 1986).

Although the solution obtained in (48) is quite simple, no explicit closed form solution has been found in the literature for the general case discussed in this example. Only the solution to the special case of an orthotropic plate weaken by a circular hole was presented (Lekhnitskii, 1968). The comparison with this special case will be shown later. In addition, in Section 7 we will also reduce our solution to the interesting case of cracks just by letting the minor axis of the ellipse to zero.

5.1. Moments around the hole boundary

According to the relations obtained in Section 3, we know that to obtain the explicit solutions for the moments around the elliptical hole boundary, the first step we need to do is calculating $\boldsymbol{\phi}_{,s}$ and $\boldsymbol{\phi}_{,n}$. Differentiation with respect to s and n can be achieved by using the chain rule,

$$\frac{\partial f}{\partial s}=\frac{\partial f}{\partial \varsigma_k}\frac{\partial \varsigma_k}{\partial \psi}\frac{\partial \psi}{\partial z_k}\left(\frac{\partial z_k}{\partial x}\frac{\partial x}{\partial s}+\frac{\partial z_k}{\partial y}\frac{\partial y}{\partial s}\right),$$
$$\frac{\partial f}{\partial n}=\frac{\partial f}{\partial \varsigma_k}\frac{\partial \varsigma_k}{\partial \psi}\frac{\partial \psi}{\partial z_k}\left(\frac{\partial z_k}{\partial x}\frac{\partial x}{\partial n}+\frac{\partial z_k}{\partial y}\frac{\partial y}{\partial n}\right), \tag{49}$$

where $\varsigma_k = e^{i\psi}$, $\partial\varsigma_k/\partial\psi = ie^{i\psi}$, $\partial z_k/\partial\psi = -\rho(\sin\theta - \mu_k\cos\theta)$, $\partial z_k/\partial x = 1$, $\partial z_k/\partial y = \mu_k$, $\partial x/\partial s = -\sin\theta$, $\partial y/\partial s = \cos\theta$, $\partial x/\partial n = \cos\theta$, $\partial y/\partial n = \sin\theta$ along the hole boundary, and ρ is defined as

$$\rho = \sqrt{a^2\sin^2\psi + b^2\cos^2\psi}, \tag{50a}$$

where the angle θ is related to the parameter ψ by

$$\rho\cos\theta = b\cos\psi, \quad \rho\sin\theta = a\sin\psi. \tag{50b}$$

By using (49), we obtain

$$\frac{\partial\varsigma_k^{-1}}{\partial s} = -\frac{i}{\rho}e^{-i\psi} = -\left(\frac{1}{a}\sin\theta + \frac{i}{b}\cos\theta\right), \tag{51a}$$

$$\frac{\partial\varsigma_k^{-1}}{\partial n} = \frac{i}{\rho}e^{-i\psi}\mu_k\left(\theta-\frac{\pi}{2}\right) = \left(\frac{1}{a}\sin\theta + \frac{i}{b}\cos\theta\right)\mu_k\left(\theta-\frac{\pi}{2}\right), \tag{51b}$$

along the hole boundary.

By using the results of differentiation obtained in (51a) and (51b) and the identities proved in (36a)–(36c), the differentiation of the stress function vector $\boldsymbol{\phi}$ with respect to s and n can be obtained as

$$\boldsymbol{\phi}_{,s} = 0, \tag{52a}$$

$$\begin{aligned}\boldsymbol{\phi}_{,n} = &-\widehat{M}_x\left\{\cos\theta\,\mathbf{E}_1\left(\theta-\frac{\pi}{2}\right) + \sin\theta\left[\mathbf{I} + \frac{b}{a}\mathbf{F}_1\left(\theta-\frac{\pi}{2}\right)\right]\right\}\mathbf{i}_2\\ &+\widehat{M}_y\left\{\sin\theta\,\mathbf{E}_1\left(\theta-\frac{\pi}{2}\right) - \cos\theta\left[\mathbf{I} + \frac{a}{b}\mathbf{F}_1\left(\theta-\frac{\pi}{2}\right)\right]\right\}\mathbf{i}_1,\end{aligned} \tag{52b}$$

where $\mathbf{E}_1(\theta)$ and $\mathbf{F}_1(\theta)$ and are defined in (37), which are matrices composed of the fundamental real matrices $\mathbf{N}_i(\theta)$, $\mathbf{S}$, $\mathbf{H}$ and $\mathbf{L}$ whose explicit expressions have been found in (Hsieh and Hwu, 2002a).

With the results of (52a) and (52b), the moments around the hole boundary can then be calculated easily from (22a), (22b) and (24).

5.2. Circular holes

For an anisotropic plate weakened by a circular hole with radius a subjected to $M_x = \widehat{M}$, $M_y = M_{xy} = 0$, the explicit solution (48) can be reduced to

$$\boldsymbol{\phi} = \boldsymbol{\phi}^\infty - a\widehat{M}\,\mathrm{Im}\{\mathbf{A}\langle\varsigma_k^{-1}\rangle\mathbf{A}^{-1}\}\mathbf{i}_2, \tag{53a}$$

$$\boldsymbol{\alpha} = \boldsymbol{\alpha}^\infty - a\widehat{M}\,\mathrm{Im}\{\mathbf{B}\langle\varsigma_k^{-1}\rangle\mathbf{A}^{-1}\}\mathbf{i}_2, \tag{53b}$$

and (47b) becomes

$$\mathbf{w}'(z) = \frac{1}{2d}\left\{\begin{array}{c} \dfrac{\mathrm{i}a\widehat{M}h_2}{c_1\varsigma_1} \\ \dfrac{-\mathrm{i}a\widehat{M}h_1}{c_2\varsigma_2} \end{array}\right\}. \tag{53c}$$

If the plate is composed of orthotropic materials with thickness h, the bending stiffness D_{ij} will be

$$D_{11} = \frac{E_1h^3}{12(1-v_1v_2)}, \quad D_{22} = \frac{E_2h^3}{12(1-v_1v_2)}, \quad D_{12} = v_1D_{22} = v_2D_{11}, \quad D_{16} = D_{26} = 0, \quad D_{66} = \frac{Gh^3}{12}, \tag{54a}$$

where E_1 and E_2 are the Young's moduli in x_1 and x_2 directions, respectively; G is the shear modulus in the x_1x_2 plane; v_1 and v_2 are the major and minor Poisson's ratios, respectively, and satisfy

$$\frac{v_1}{E_1} = \frac{v_2}{E_2}. \tag{54b}$$

With the use of (54a), (54b) and (12b), $\mathbf{w}'(z)$ given in (53c) can now be written explicitly as

$$\mathbf{w}'(z) = \left\{\begin{array}{c} \dfrac{1}{2c_1}\dfrac{\mathrm{i}(v_1+\mu_2^2)}{D_{11}(\mu_2-\mu_1)\left[\frac{v_1-n^2}{k}+1+v_1v_2+kv_2\right]}\dfrac{\widehat{M}a}{\zeta_1} \\ \dfrac{1}{2c_2}\dfrac{-\mathrm{i}(v_1+\mu_1^2)}{D_{11}(\mu_2-\mu_1)\left[\frac{v_1-n^2}{k}+1+v_1v_2+kv_2\right]}\dfrac{\widehat{M}a}{\zeta_2} \end{array}\right\}, \tag{55a}$$

where

$$k = -\mu_1\mu_2 = \sqrt{\frac{D_{11}}{D_{22}}}, \quad n = -\mathrm{i}(\mu_1+\mu_2). \tag{55b}$$

With the results of (55a) and (55b), the deflection w can easily be obtained from (2) by simple integration, which can be proved to be identical to that shown in Lekhnitskii (1968).

6. Elliptical inclusions

Consider an unbounded anisotropic plate embedded with a rigid elliptical inclusion subjected to out-of-plane bending moments $M_x = \widehat{M}_x$, $M_y = \widehat{M}_y$, and $M_{xy} = 0$ at infinity. In this case we are dealing with a second fundamental problem of elasticity due to the fact that the deformation is specified at the contour of the inclusion. Since the rigid inclusion cannot undergo deformation, the boundary conditions of this problem can be expressed as

$$M_x = \widehat{M}_x, \quad M_y = \widehat{M}_y, \quad M_{xy} = 0 \quad \text{at infinity}, \tag{56a}$$

$$w = \frac{\partial w}{\partial n} = 0 \quad \text{along the inclusion boundary}. \tag{56b}$$

From the discussions of Hwu (2002a), we know that the boundary condition (56a) and (56b) can also be expressed in terms of the stress function vector $\boldsymbol{\phi}$ and slope vector $\boldsymbol{\alpha}$ as

$$\boldsymbol{\phi} = -\widehat{M}_xy\mathbf{i}_2 - \widehat{M}_yx\mathbf{i}_1 \quad \text{at infinity}, \tag{57a}$$

$$\boldsymbol{\alpha} = 0 \quad \text{along the inclusion boundary.} \tag{57b}$$

By referring to the corresponding two-dimensional problems (Hwu and Ting, 1989; Hwu and Yen, 1993) and using the approach similar to the previous section, we obtain the explicit solution for the inclusion problems as

$$\mathbf{w}'(z) = \frac{1}{2}\langle\zeta_k^{-1}\rangle\mathbf{B}^{-1}\left[a\left(\widehat{M}_x\mathbf{d}_1 + \widehat{M}_y\mathbf{d}_3\right) - \mathrm{i}b\left(\widehat{M}_x\mathbf{d}_2 + \widehat{M}_y\mathbf{d}_4\right)\right], \tag{58a}$$

$$\boldsymbol{\phi} = \boldsymbol{\phi}^\infty + \mathrm{Re}\left\{\mathbf{A}\langle\zeta_k^{-1}\rangle\mathbf{B}^{-1}\left[a\left(\widehat{M}_x\mathbf{d}_1 + \widehat{M}_y\mathbf{d}_3\right) - \mathrm{i}b\left(\widehat{M}_x\mathbf{d}_2 + \widehat{M}_y\mathbf{d}_4\right)\right]\right\}, \tag{58b}$$

$$\boldsymbol{\alpha} = \boldsymbol{\alpha}^\infty + \mathrm{Re}\left\{\mathbf{B}\langle\zeta_k^{-1}\rangle\mathbf{B}^{-1}\left[a\left(\widehat{M}_x\mathbf{d}_1 + \widehat{M}_y\mathbf{d}_3\right) - \mathrm{i}b\left(\widehat{M}_x\mathbf{d}_2 + \widehat{M}_y\mathbf{d}_4\right)\right]\right\}, \tag{58c}$$

where $\boldsymbol{\phi}^\infty$ and $\boldsymbol{\alpha}^\infty$ are given in (42a) and (42b).

Note that from the boundary conditions shown in (56b) or (57b), it seems that the rigid body motion of the rigid inclusion has been suppressed. Actually, the rigid inclusion is allowed to move in space and rotate. The rigid body translation and the rotation about the z-axis will lead to $\boldsymbol{\alpha} = 0$, while the rigid body rotation about the x-axis and y-axis will lead to $\boldsymbol{\alpha} = \text{constant}$. From the Stroh-like formalism (5) and the relations for the moments and transverse shear forces given in (22a)–(27), we know that constant term of $\boldsymbol{\alpha}$ will not have contribution to the internal stresses of the plates and hence can be neglected in our calculation.

6.1. Moments around the inclusion boundary

Similar to Section 5, the vectors of $\boldsymbol{\phi}_{,s}$ and $\boldsymbol{\phi}_{,n}$ around the inclusion boundary can be obtained as

$$\begin{aligned}\boldsymbol{\phi}_{,s} = {} & -\widehat{M}_x\cos\theta\mathbf{i}_2 + \widehat{M}_y\sin\theta\mathbf{i}_1 + \left(\sin\theta\mathbf{S}\mathbf{L}^{-1} - \frac{a}{b}\cos\theta\mathbf{L}^{-1}\right)\left(\widehat{M}_x\mathbf{d}_1 + \widehat{M}_y\mathbf{d}_3\right) \\ & + \left(\cos\theta\mathbf{S}\mathbf{L}^{-1} + \frac{b}{a}\sin\theta\mathbf{L}^{-1}\right)\left(\widehat{M}_x\mathbf{d}_2 + \widehat{M}_y\mathbf{d}_4\right),\end{aligned} \tag{59a}$$

$$\begin{aligned}\boldsymbol{\phi}_{,n} = {} & -\widehat{M}_x\sin\theta\mathbf{i}_2 - \widehat{M}_y\cos\theta\mathbf{i}_1 + \left[\sin\theta\mathbf{E}_2\left(\theta - \frac{\pi}{2}\right) - \frac{a}{b}\cos\theta\mathbf{F}_2\left(\theta - \frac{\pi}{2}\right)\right]\left(\widehat{M}_x\mathbf{d}_1 + \widehat{M}_y\mathbf{d}_3\right) \\ & + \left[\cos\theta\mathbf{E}_2\left(\theta - \frac{\pi}{2}\right) + \frac{b}{a}\sin\theta\mathbf{F}_2\left(\theta - \frac{\pi}{2}\right)\right]\left(\widehat{M}_x\mathbf{d}_2 + \widehat{M}_y\mathbf{d}_4\right),\end{aligned} \tag{59b}$$

where $\mathbf{E}_2(\theta)$ and $\mathbf{F}_2(\theta)$ are defined in (37). With the results of (59a) and (59b), the moments around the inclusion boundary can then be calculated from (22a), (22b) and (24).

6.2. Circular inclusions

For an anisotropic plate embedded with a rigid circular inclusion with radius a subjected to $M_x = \widehat{M}$, $M_y = M_{xy} = 0$, the explicit solution (58a)–(58c) can be reduced to

$$\mathbf{w}'(z) = \frac{1}{2}a\widehat{M}\langle\varsigma_k^{-1}\rangle\mathbf{B}^{-1}(\mathbf{d}_1 - \mathrm{i}\mathbf{d}_2), \tag{60a}$$

$$\boldsymbol{\phi} = \boldsymbol{\phi}^\infty + a\widehat{M}\mathrm{Re}\left\{\mathbf{A}\langle\varsigma_k^{-1}\rangle\mathbf{B}^{-1}(\mathbf{d}_1 - \mathrm{i}\mathbf{d}_2)\right\}, \tag{60b}$$

$$\boldsymbol{\alpha} = \boldsymbol{\alpha}^\infty + a\widehat{M}\mathrm{Re}\left\{\mathbf{B}\langle\varsigma_k^{-1}\rangle\mathbf{B}^{-1}(\mathbf{d}_1 - \mathrm{i}\mathbf{d}_2)\right\}. \tag{60c}$$

If the plate is orthotropic, then

$$D^*_{11} = \frac{D_{22}}{D_{11}D_{22} - D^2_{12}}, \quad D^*_{22} = \frac{D_{11}}{D_{11}D_{22} - D^2_{12}}, \quad D^*_{12} = \frac{D_{22}}{D_{11}D_{22} - D^2_{12}}, \quad D^*_{16} = D^*_{26} = 0, \quad D^*_{66} = \frac{1}{D_{66}}, \tag{61}$$

where D_{ij} are given in (54a). Substituting (10), (12a)–(12c), (42b), (54a), (54b) and (61) into (60a), $\mathbf{w}'(z)$ can then be reduced to

$$\mathbf{w}'(z) = \begin{Bmatrix} -\dfrac{\mu_2 + \mathrm{i}v_1}{2c_1(\mu_1 - \mu_2)D_{11}(1 - v_1v_2)} \dfrac{\widehat{M}a}{\varsigma_1} \\ \dfrac{\mu_1 + \mathrm{i}v_1}{2c_2(\mu_1 - \mu_2)D_{11}(1 - v_1v_2)} \dfrac{\widehat{M}a}{\varsigma_2} \end{Bmatrix}, \tag{62}$$

which is exactly the same as that shown in Lekhnitskii (1968).

7. Moment intensity factors for crack problems

An elliptic opening can be made into a crack of length $2a$ by letting the minor axis b be zero. The explicit solution given in (48) is then applicable to crack problem with $b = 0$. Consider a cracked plate subjected to bending moment $M_y = \widehat{M}_y$ at infinity. The stress function vector $\boldsymbol{\phi}$ and the slope vector $\boldsymbol{\alpha}$ of this problem may therefore be obtained from (48) with $b = \widehat{M}_x = 0$, i.e.,

$$\boldsymbol{\phi} = \boldsymbol{\phi}^{\infty} + a\widehat{M}_y \mathrm{Re}\{\mathbf{A}\langle\varsigma_k^{-1}\rangle\mathbf{A}^{-1}\}\mathbf{i}_1, \tag{63a}$$

$$\boldsymbol{\alpha} = \boldsymbol{\alpha}^{\infty} + a\widehat{M}_y \mathrm{Re}\{\mathbf{B}\langle\varsigma_k^{-1}\rangle\mathbf{A}^{-1}\}\mathbf{i}_1, \tag{63b}$$

where

$$\boldsymbol{\phi}^{\infty} = -\widehat{M}_y x\mathbf{i}_1, \quad \boldsymbol{\alpha}^{\infty} = \widehat{M}_y(\mathbf{d}_4 y - \mathbf{d}_3 x), \quad \varsigma_k = \frac{1}{a}\left(z_k + \sqrt{z_k^2 - a^2}\right). \tag{63c}$$

For the crack problem, it is interesting to know the moment intensity factors which is usually defined as

$$\mathbf{K} = \begin{Bmatrix} K_{\mathrm{I}} \\ K_{\mathrm{II}} \end{Bmatrix} = \frac{6}{h^2}\lim_{r\to 0}\sqrt{2\pi r}\begin{Bmatrix} M_y(r) \\ M_{xy}(r) \end{Bmatrix}, \tag{64}$$

where r is the distance ahead of the crack tip. Thus, to find the moment intensity factors, we need to calculate M_y, M_{xy} ahead of the crack tip. To calculate the moments ahead of the crack tip, we may use the relations given in (15, part 2) and (16), and let $x = a + r$, $y = 0$. The differentiation with respect to x and y can be performed by using chain rule, i.e.,

$$\frac{\partial\varsigma_k^{-1}}{\partial x} = \frac{\partial\varsigma_k^{-1}}{\partial\varsigma_k}\frac{\partial\varsigma_k}{\partial z_k}\frac{\partial z_k}{\partial x} = \frac{1}{a}\left(1 - \frac{z_k}{\sqrt{z_k^2 - a^2}}\right), \qquad \frac{\partial\varsigma_k^{-1}}{\partial y} = \frac{\partial\varsigma_k^{-1}}{\partial\varsigma_k}\frac{\partial\varsigma_k}{\partial z_k}\frac{\partial z_k}{\partial y} = \frac{\mu_k}{a}\left(1 - \frac{z_k}{\sqrt{z_k^2 - a^2}}\right). \tag{65}$$

Using the results of (65) and considering the near tip range $y = 0$, $x = a + r$, where $r \to 0$, and with the help of the identity (32, part 1), the differentiation of the stress function vector $\boldsymbol{\phi}$ in (63a) with respect to x and y, may lead to

$$\boldsymbol{\phi}_{,x} = -\sqrt{\frac{a}{2r}}\widehat{M}_y\mathbf{i}_1, \qquad \boldsymbol{\phi}_{,y} = -\sqrt{\frac{a}{2r}}\widehat{M}_y\mathbf{E}_1\mathbf{i}_1. \tag{66}$$

With (66), the moments M_y and M_{xy} near the crack tip may then be obtained from (15, part 2) and (16). Substituting their near tip values into the definition (64), we obtain the moment intensity factor as

$$K_{\mathrm{I}} = \frac{6}{h^2}\sqrt{\pi a}\widehat{M}_y, \tag{67a}$$

$$K_{\mathrm{II}} = -\frac{3}{h^2}\sqrt{\pi a}\widehat{M}_y(\mathbf{E}_1)_{11}. \tag{67b}$$

From (67a) and (67b), we see that the moment intensity factor K_{II} not only depends on its geometry but also depends on its material properties, and K_{I}, K_{II} increase as the crack length $2a$ increases or plate thickness h decreases.

If the plate is made of orthotropic materials, $\mathbf{N}_1$, $\mathbf{N}_2$, $\mathbf{S}$, $\mathbf{H}$ have the following structures, which can be seen from (11) and (Hsieh and Hwu, 2002a),

$$\mathbf{N}_1 = \begin{bmatrix} 0 & -1 \\ * & 0 \end{bmatrix}, \quad \mathbf{N}_2 = \begin{bmatrix} * & 0 \\ 0 & * \end{bmatrix}, \quad \mathbf{S} = \begin{bmatrix} 0 & * \\ * & 0 \end{bmatrix}, \quad \mathbf{H} = \begin{bmatrix} * & 0 \\ 0 & * \end{bmatrix}. \tag{68}$$

Plugging this information into the definition of $\mathbf{E}_1$ given in (37), it can easily be proved that

$$(\mathbf{E}_1)_{11} = 0, \quad \text{for orthotropic plates.} \tag{69}$$

Thus, mode II moment intensity factor equals to zero for cracks in orthotropic plates subjected to bending moments $\widehat{M}_y$ at infinity.

8. Numerical examples

To show that the explicit solutions obtained in (52a) and (52b) for the moments around the hole boundary, and (59a) and (59b) for the moments around the inclusion boundary are exact, several examples are illustrated in this section. All the examples shown in this section consider an unbounded carbon-epoxy plate (T300/N5208) containing a hole or a rigid inclusion. The plate thickness is $h = 3$ mm, and the material properties of the carbon-epoxy are

$$E_1 = 181 \text{ GPa}, \quad E_2 = 10.3 \text{ GPa}, \quad G = 7.17 \text{ GPa}, \quad v_1 = 0.28.$$

The bending stiffnesses calculated by using the materials properties and the plate thickness are

$$D_{11} = 409.08, \quad D_{22} = 23.28, \quad D_{12} = 6.52, \quad D_{16} = D_{26} = 0, \quad D_{66} = 16.13. \ (\text{GPa}\,\text{mm}^3)$$

With the eigen-relation (7a)–(7c), the material eigenvalues are obtained as

$$\mu_1 = 1.1239 + 1.7114\text{i}, \quad \mu_2 = -1.1239 + 1.7114\text{i}.$$

Substituting these data into (11), (31), (33a), (33b) and (33c), the matrices $\mathbf{N}_i$, $\mathbf{N}_i(\theta)$, $\mathbf{S}$, $\mathbf{H}$ and $\mathbf{L}$ can easily be obtained. Note that instead of calculating $\mathbf{S}$, $\mathbf{H}$ and $\mathbf{L}$ through the eigenvector matrices, their explicit expressions in terms of bending stiffness can be found in Hsieh and Hwu (2002a).

Table 1
Moments around the circular hole of an orthotropic carbon-epoxy plate subjected to out-of-plane bending moments $M_x = \widehat{M}$, $M_y = M_{xy} = 0$

Angle (ψ)	Moments			
	$M_{nt}/\widehat{M}$		$M_t/\widehat{M}$	
	Present	Lekhnitskii (1968)	Present	Lekhnitskii (1968)
0°	0	0	0.1370	0.1369
15°	−0.0316	−0.0316	0.1508	0.1507
30°	−0.0871	−0.0871	0.2112	0.2112
45°	−0.2145	−0.2146	0.4170	0.4170
60°	−0.4877	−0.4876	1.1192	1.1193
75°	−0.5914	−0.5913	2.5062	2.5062
90°	0	0	3.0568	3.0566

Due to symmetry, only a quarter of the circular hole is presented.

Table 2
Moments around the circular inclusion of an orthotropic carbon-epoxy plate subjected to out-of-plane bending moments $M_x = \widehat{M}$, $M_y = M_{xy} = 0$

Angle (ψ)	Moments			
	$M_n/\widehat{M}$		$M_{nt}/\widehat{M}$	$M_t/\widehat{M}$
	Present	Lekhnitskii (1968)	Present	Present
0°	1.8918	1.8918	0	0.0302
15°	1.7443	1.7443	−0.4185	0.1386
30°	1.3412	1.3412	−0.6645	0.3981
45°	0.7907	0.7907	−0.5982	0.5906
60°	0.2401	0.2401	−0.2036	0.3297
75°	−0.1629	−0.1629	0.0593	−0.1735
90°	−0.3104	−0.3104	0	−0.0869

Due to symmetry, only a quarter of the circular inclusion is presented.

8.1. Example 1: A circular hole or rigid inclusion in an orthotropic plate

The purpose of this example is to verify our results by using the existing solutions obtained in Lekhnitskii (1968) for the present special conditions. Although the deflection functions for these special cases shown in (55a), (55b) and (62) have been verified analytically, their associated moments distributions such as those shown in (52a), (52b), (59a) and (59b) have not been checked. By using the numerical data shown above for the orthotropic plate, and employing (52a), (52b), (59a), (59b), (22a), (22b) and (24), the moments around the circular hole/inclusion boundary are presented in Tables 1 and 2, which show that our solutions are almost the same as those obtained in Lekhnitskii (1968). Note that in Table 2, only M_n is checked because no formulae for M_t and M_{nt} were provided in (Lekhnitskii, 1968) due to their complexity.

8.2. Example 2: A circular hole or rigid inclusion in an anisotropic plate

After verifying our solutions by using the existing solutions for the special cases, in order to show the generality of our solutions we now consider the anisotropic plates. The anisotropy of the plate is made by orienting the fiber direction of carbon-epoxy counterclockwise from x-axis to 30° or 60°. Figs. 3 and 4 show the moment distributions around the circular hole/inclusion boundary for four different fiber orientations, 0°, 30°, 60° and 90°. One interesting result shown in Fig. 3 is that the maximum value of M_t always occurs at the location perpendicular to the fiber direction when the applied moment $\widehat{M}_x$ remains parallel to the x-axis.

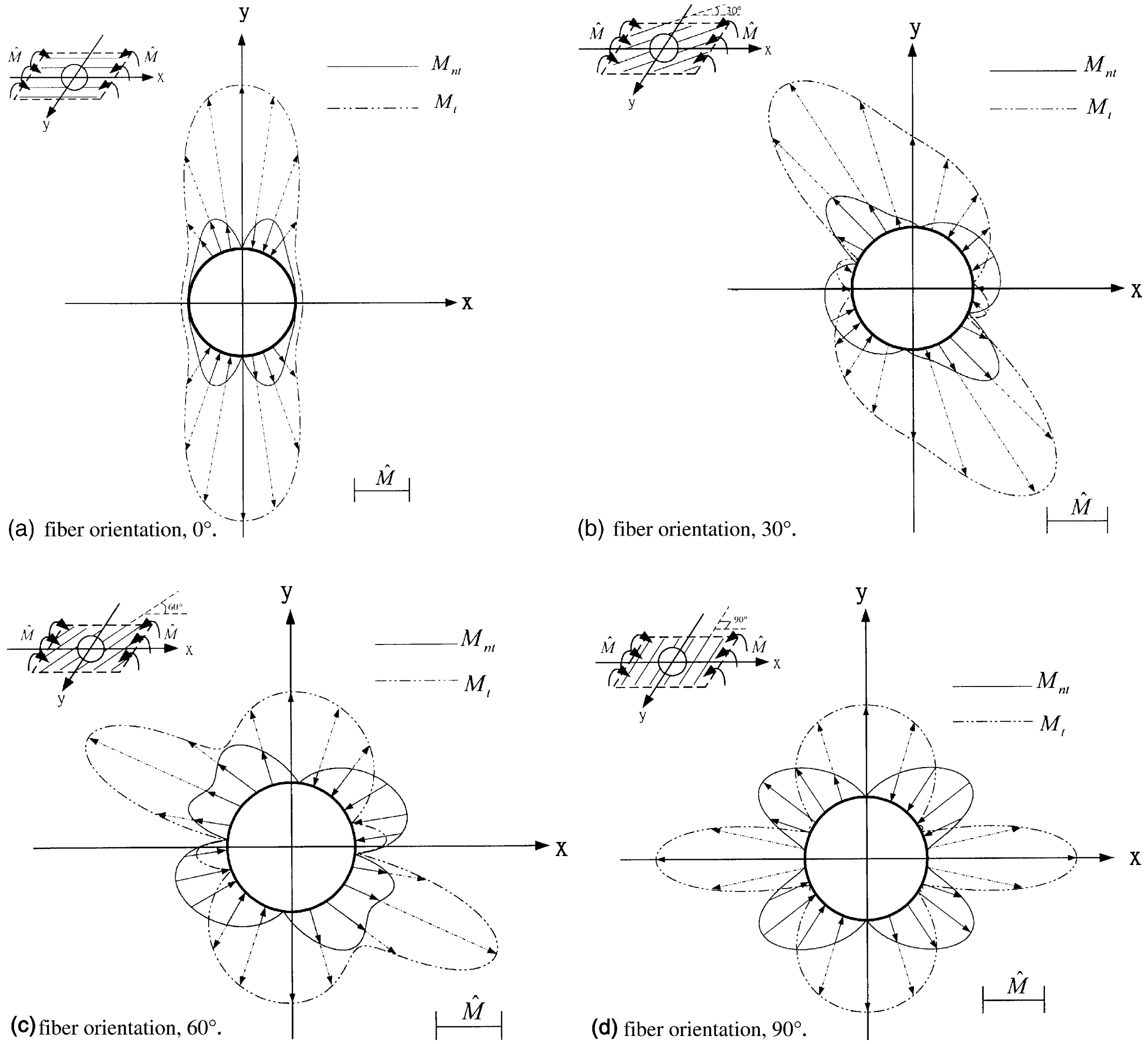

Fig. 3. Moments around the circular hole in an anisotropic plate, fiber orientation: (a) 0°, (b) 30°, (c) 60° and (d) 90°.

Moreover, the maximum value of M_t decreases when the fiber orientation increases. Similar situation does not occur in M_{nt} of circular holes and all the moment components of circular inclusions.

8.3. Example 3: An elliptical hole or rigid inclusion in an anisotropic plate

Example 2 shows the effects of material properties on the moment distributions around the hole/inclusion boundary. Because our solutions obtained in this paper are also valid for the general elliptical shape, it is interesting to know the effects of hole/inclusion shapes by just changing the ratio of minor axis to major axis. Consider the anisotropic plates with fiber oriented counterclockwise 30° from x-axis. Figs. 5 and 6 show moment M_t around hole/inclusion boundary versus angle ψ for five different ratios, $b/a = 5$, 2, 1, 1/2, 1/5. From Fig. 5 we see that for hole problems, the maximum value of M_t increases when the ratio

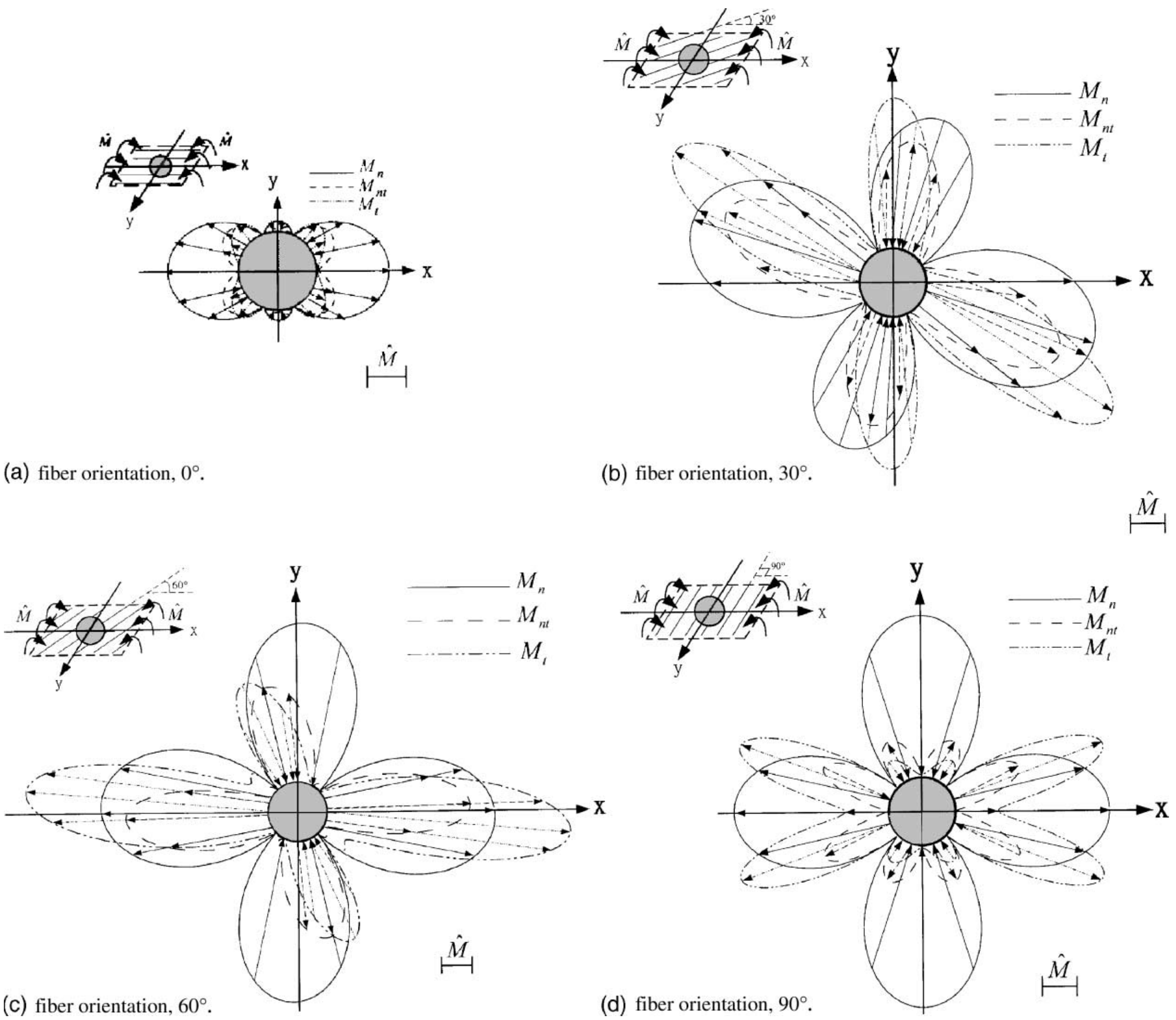

Fig. 4. Moments around the circular rigid inclusion in an anisotropic plate, fiber orientation: (a) 0°, (b) 30°, (c) 60° and (d) 90°.

b/a increases. Moreover, the location of the maximum value of M_t will also move away from the location perpendicular to the fiber direction if the ratio is away from unity (a circle). Note that for higher ratio such as $b/a = 5$ the elliptic hole may approach to a crack perpendicular to the applied moments $\widehat{M}_x$. Therefore, the maximum value of M_t may approach to infinity if the ratio approaches to infinity. On the other hand, if the ratio b/a approaches to zero, the elliptical hole may approach to a crack parallel to the applied moment. According to the moment intensity factors obtained in (67a) and (67b), we know $\widehat{M}_x$ will not influence the intensity of the near tip stresses, which may also explain why the maximum value of M_t decreases when the ratio b/a decreases.

The results presented in Fig. 6 for the inclusion problems show that the narrower the inclusion the higher the maximum value of M_t no matter the inclusion is perpendicular or parallel to the applied moment. The location of the maximum value of M_t will approach to 90° (or 270°) when b/a increases, and approach to 0° (or 180° or 360°) when b/a decreases, which is reasonable.

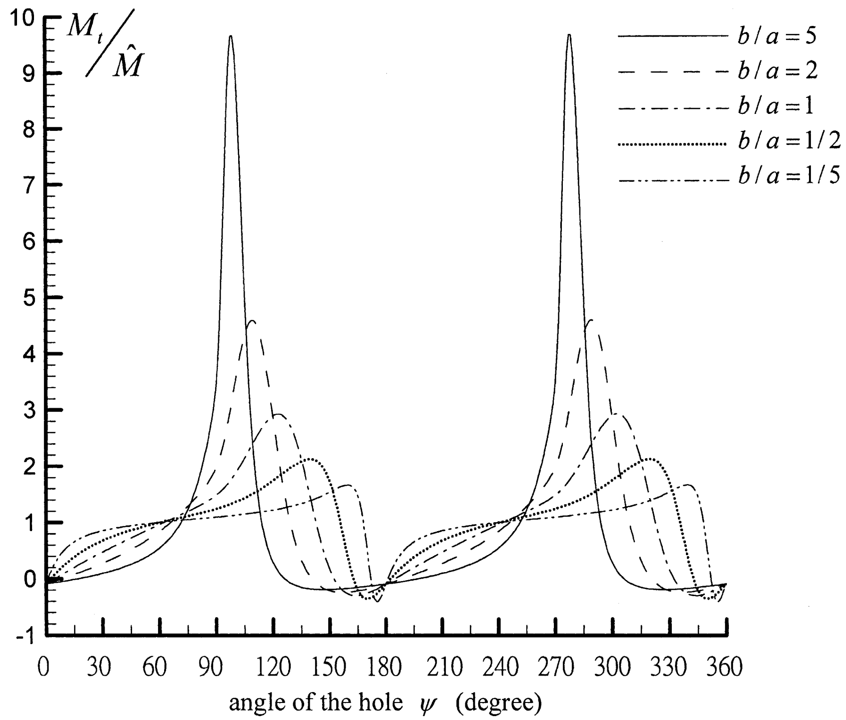

Fig. 5. Moments around the elliptical hole in an anisotropic plate (fiber orientation, 30°; $M_x = \widehat{M}$, $M_y = M_{xy} = 0$).

In Fig. 5, we shows the plot of M_t instead of M_{nt} because the location of M_{nt} does not have the rules like M_t, but the maximum value of M_{nt} will also approach to infinity if the ratio b/a approaches to infinity.

9. Conclusions

The explicit closed form solutions for an anisotropic plate containing an elliptical hole or rigid inclusion subjected to out-of-plane bending moments are obtained by applying the Stroh-like formalism for plate bending problems. The solutions for the crack problems are obtained by letting the minor axis of the ellipse approach to zero and the moment intensity factors of the cracks are also obtained. To verify their correctness and to show their generality, several examples are presented. Because the analytical solutions existing in the literature are valid only for the orthotropic plates containing a circular hole or a rigid inclusion, the comparison can only be made for this special case. The results show that our solutions are identical to those obtained in the literature for this special case. Beyond this special case, our solutions also cover general anisotropic materials with elliptical holes or inclusions or cracks, which have not been found in the literature.

One should note that the Stroh-like formalism introduced in this paper considers only the plate bending problems. Therefore, if one considers the general laminated composites, this formalism may not be applicable due to the possible coupling between bending and in-plane deformation. Only when the laminates are symmetric with respect to the mid-plane, the bending and in-plane deformations are decoupled and the present results can be utilized. If one is interested in the coupled stretching–bending analysis for the general non-symmetric laminates, please refer to one of the author's recent paper (Hwu, 2002b) and our upcoming paper (Hsieh and Hwu, 2002b) for the coupled stretching–bending analysis for holes in laminates.

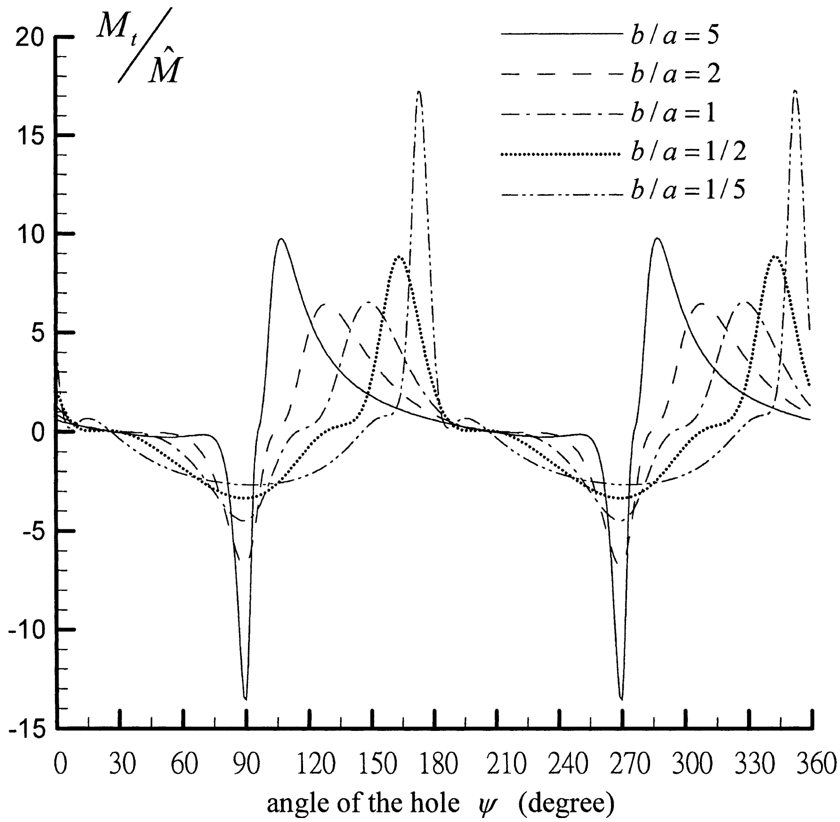

Fig. 6. Moments around the elliptical rigid inclusion in an anisotropic plate (fiber orientation, 30°; $M_x = \widehat{M}$, $M_y = M_{xy} = 0$).

One other restriction mentioned in this paper is that the material eigenvalues should be distinct. If the material eigenvalues are repeated, such as the very common cases of isotropic plates, the solutions presented in this paper should be modified. This modification has been discussed vastly in the two-dimensional problems. Due to the similarity between the Stroh-like formalism and the Stroh formalism, same techniques developed in two-dimensional problems can be transferred to the present problems directly without any difficulties. If one only wants to use the present formulae to calculate the related numerical values, no modification is required because all the problems caused by the repeated eigenvalues can be avoided just by introducing a small perturbation in the values of the material eigenvalues or the material properties. Moreover, if the solutions do not contain the material eigenvector matrices **A** and **B**, the problems of repeated eigenvalues will not cause any trouble to the solutions. In other words, the solutions are valid for the cases of repeated eigenvalues. For example, in this paper the moments around the hole/inclusion boundaries and the moment intensity factors are not expressed in terms of **A** and **B** but are expressed in terms of the fundamental matrices $\mathbf{N}_i(\theta)$, **S**, **H** and **L** whose explicit expressions have been found in Hsieh and Hwu (2002a).

References

Barnett, D.M., Kirchner, H.O.K., 1997. A proof of the equivalence of the Stroh and Lekhnitskii sextic equations for plane anisotropic elastostatics. Philos. Mag. A 76 (1), 231–239.

Hsieh, M.C., Hwu, C., 2002a. Explicit expressions for the fundamental elasticity matrices of Stroh-like formalism for symmetric/unsymmetric laminates, The Chin. J. Mech., Series A, in press.

Hsieh, M.C., Hwu, C., 2002b. Explicit solutions for the coupled stretching–bending problems of holes in composite laminates, submitted for publication.

Hwu, C., 1992. Polygonal holes in anisotropic media. Int. J. Solid Struct. 29 (19), 2369–2384.

Hwu, C., 1996. Correspondence relations between anisotropic and isotropic. The Chin. J. Mech. 12 (4), 483–493.

Hwu, C., 2002a. Stroh-like complex variable formalism for bending theory of anisotropic plates, submitted for publication.

Hwu, C., 2002b. Stroh-like formalism for the coupled stretching–bending analysis for composite laminates, submitted for publication.

Hwu, C., Ting, T.C.T., 1989. Two-dimensional problems of the anisotropic elastic solid with an elliptic inclusion. Quart. J. Mech. Appl. Math. 42 (4), 553–572.

Hwu, C., Yen, W.J., 1992. Plane problems for anisotropic bodies with an elliptic hole subjected to arbitrary loadings. The Chin. J. Mech. 8 (2), 123–129.

Hwu, C., Yen, W.J., 1993. On the anisotropic elastic inclusions in plane elastostatics. ASME J. Appl. Mech. 60, 626–632.

Lekhnitskii, S.G., 1938. Some problems related to the theory of bending of thin plates. Prikladnaya matematika i mekhanika II (2), 187.

Lekhnitskii, S.G., 1968. Anisotropic Plate. Gordon and Breach, London.

Lu, P., Mahrenholtz, O., 1994. Extension of the Stroh formalism to the analysis of bending of anisotropic elastic plates. J. Mech. Phys. Solids 42 (11), 1725–1741.

Suo, Z., 1990. Singularities, interfaces and cracks in dissimilar anisotropic media. Proc. R. Soc. Lon. A 427, 331–358.

Szilard, R., 1985. Theory and Analysis of Plates—Classical and Numerical Methods. Prentice-Hall, Englewood Cliffs, NJ.

Ting, T.C.T., 1996. Anisotropic Elasticity—Theory and Applications. Oxford Science Publications, New York.

Ting, T.C.T., 1999. A modified Lekhnitskii formalism a la Stroh for anisotropic elasticity and classifications of the 6×6 matrix **N**. Proc. Roy. Soc. Lon. A 455 (1981), 69–89.

Vinson, J.R., Sierakowski, R.L., 1986. The Behavior of Structures Composed of Composite Materials. Martinus Nijhoff Publishers, Dordrecht, Netherlands.

Yin, W.L., 2000a. Deconstructing plane anisotropic elasticity, Part I: The Latent structure of Lekhnitskii's formalism. Int. J. Solid Struct. 37 (38), 5257–5276.

Yin, W.L., 2000b. Deconstructing plane anisotropic elasticity, Part II: Stroh's formalism sans frills. Int. J. Solid Struct. 37 (38), 5277–5296.